Supplementary Materials for

Multiplexed Printed Sensors for In-Situ Monitoring in Bivalve Aquaculture

Shuo-En Wu[1], Napasorn Phongphaew[2], Yichen Zhai[3], Lulu Yao,[1] Hsun-Hao Hsu[4], Alan Shiller[5], Jason Azoulay[6], Tse Nga Ng[1,2] *

[1]Materials Science Engineering Program, University of California San Diego, La Jolla, CA 92093, United States.

[2]Department of Electrical and Computer Engineering, University of California San Diego, La Jolla, CA 92093, United States.

[3]Department of Mechanical and Aerospace Engineering, University of California San Diego, La Jolla, CA 92093, United States.

[4]Department of Applied Chemistry, National Yang Ming Chiao Tung University, Hsinchu 30010, Taiwan

[5]Division of Marine Science, University of Southern Mississippi, Stennis Space Center, MS 39529, United States.

[6]School of Polymer Science and Engineering, The University of Southern Mississippi, Hattiesburg, MS 39406, USA

*Corresponding email: tnn046@ucsd.edu

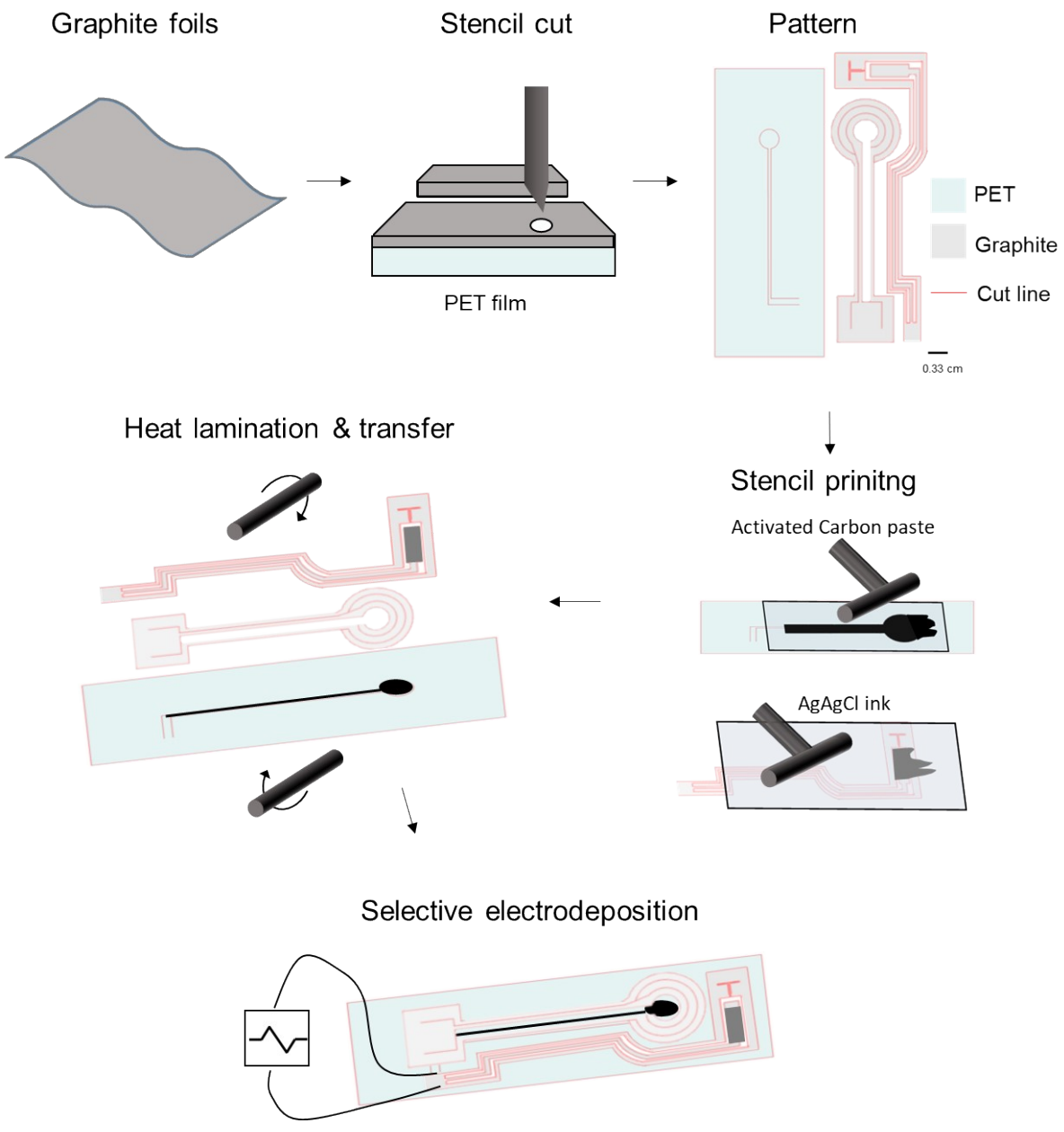

Figure S1. Fabrication flow diagram for the printed sensors.

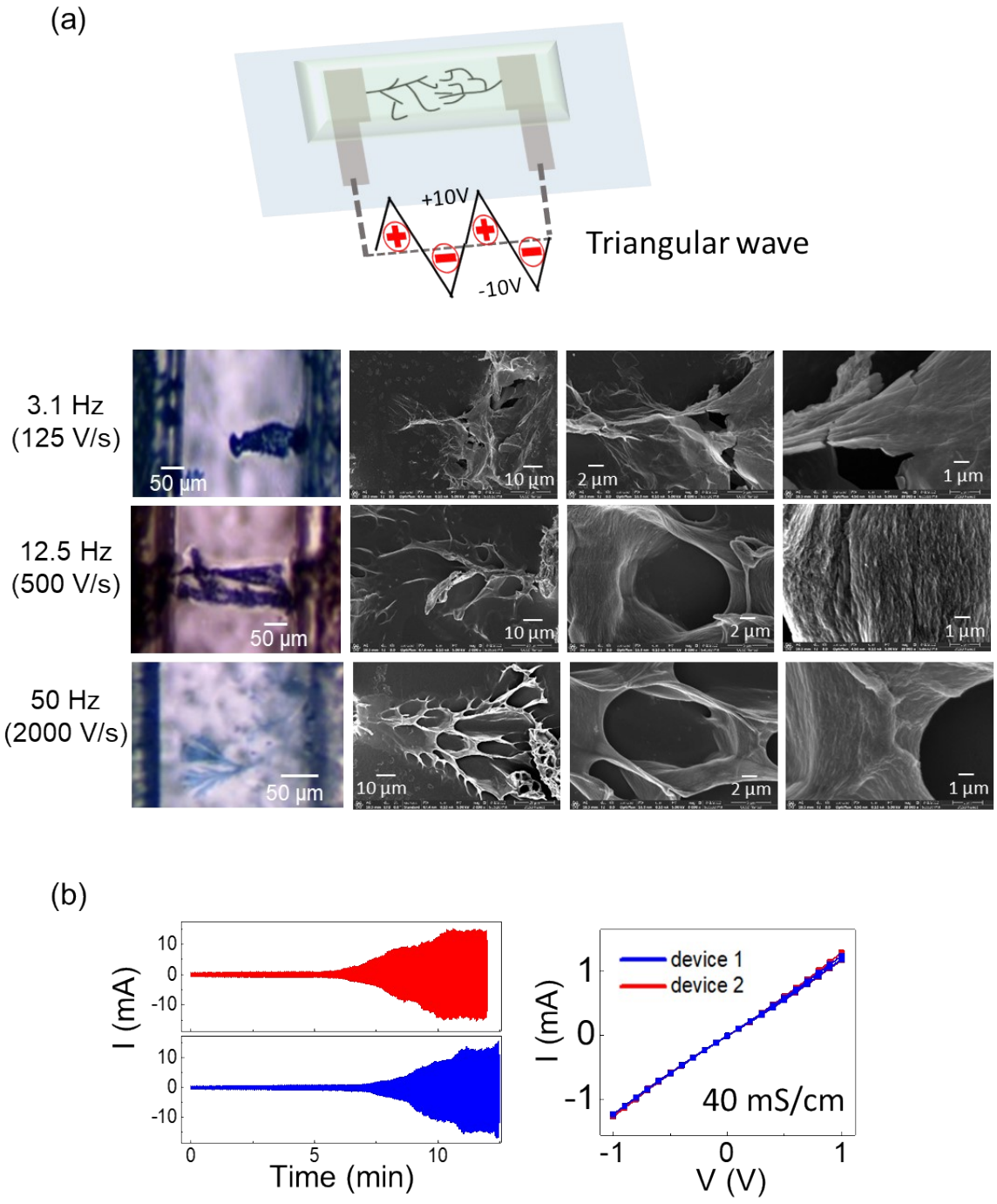

Figure S2. (a) Schematic of the AC electrodeposition waveform and photographs and scanning electron microscopy images showing the morphology of PEDOT:PF_6 deposited under different applied voltage rates. (b) Deposition current versus time for two fabrication runs, showing good reproducibility in the resulting device conductance for the two devices.

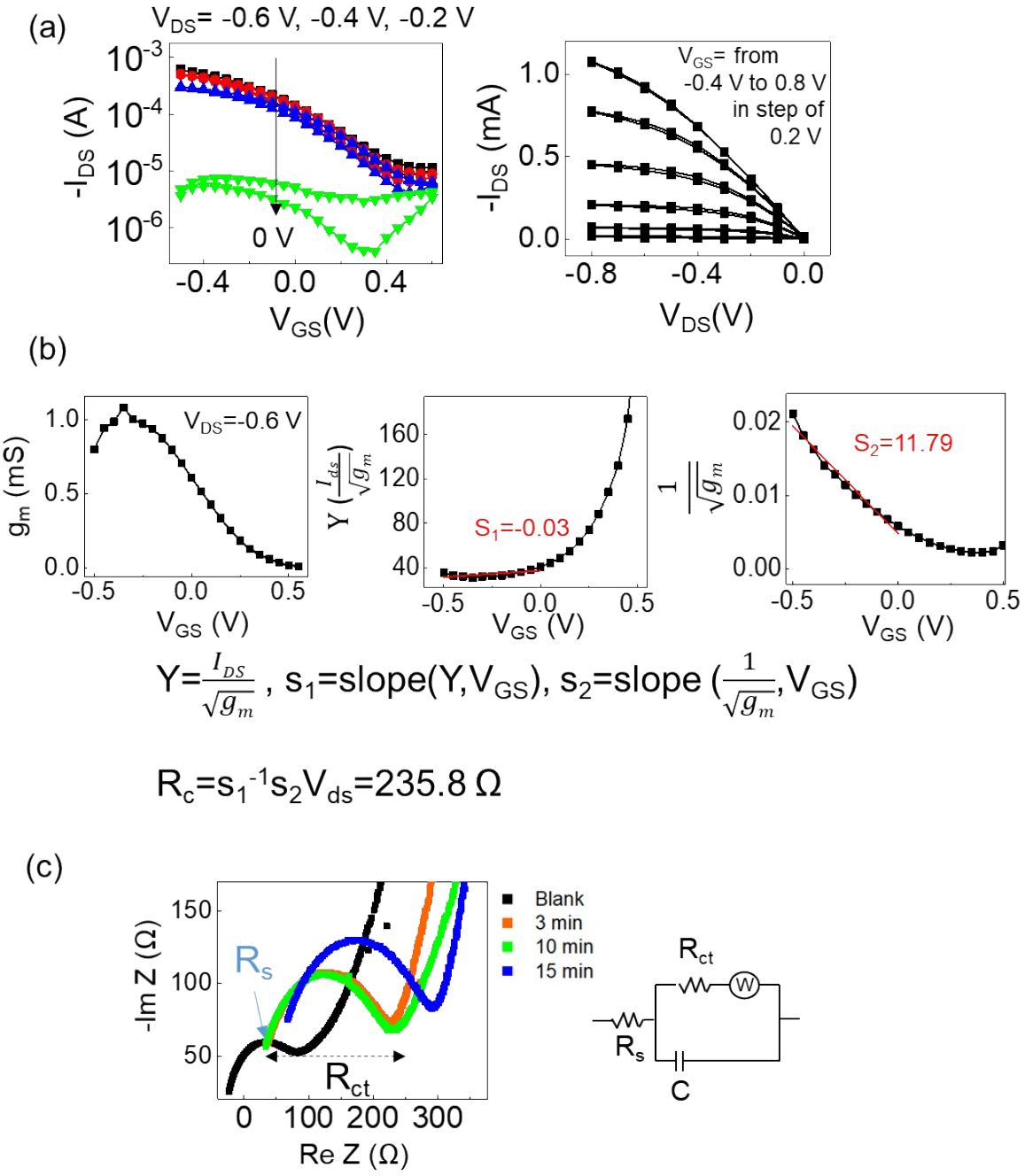

Figure S3. (a) Transfer and output characteristics of OECT in simulated seawater using Instant Ocean salt. (b) Data fitting and calculations of contact resistance of OECT through Y-function model analysis.[1] (c) Nyquist plot of PEDOT:PF_6 after different deposition periods. R_s ~50 Ohm and ~200 Ohm as read from the plot. The R_s and R_{ct} was extracted based on the Randles-Ershler equivalent circuit. Higher resistance of PEDOT:PF_6 with deposition time due to the gradual loss of PF_6 dopant in the solvent during the long deposition time.[2]

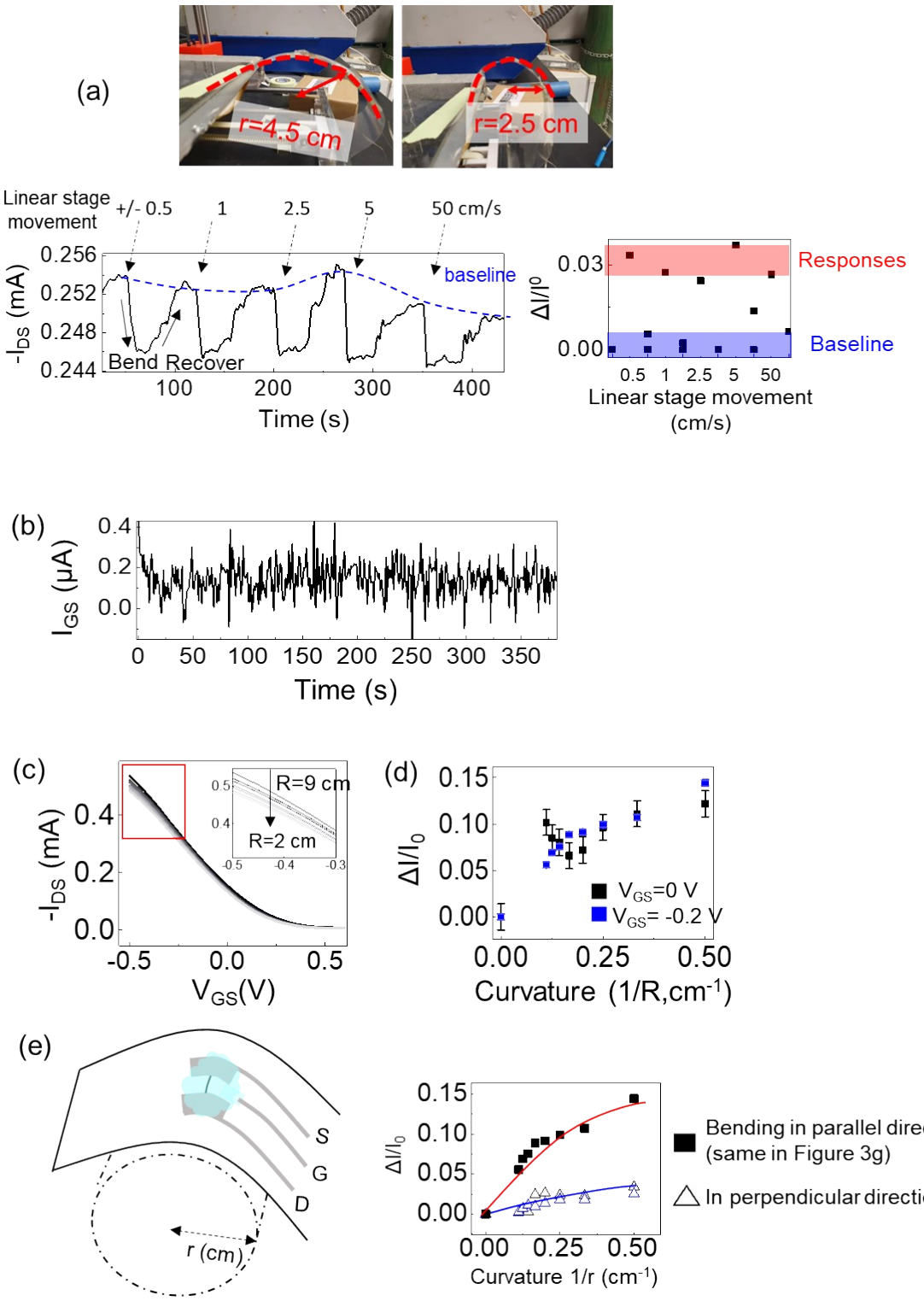

Figure S4. (a) Bending tests under different speeds, with the radii of curvature compressed from 4.5 cm to 2.5 cm as shown in the photographs. (b) Gate leakage current during bending tests in Figure 3e of the main text. (c) Transfer characteristics for calculating the transconductance in Figure 3f. (d) Normalized change in current across source-drain electrodes biased at V_{DS} = -0.5 V under different curvatures. The data in black represent operating the

device at zero gate bias, such that it was essentially a resistor without gate amplification. The device signal was not distinguishable from noise under small curvatures, while the device with amplification at V_{GS} = -0.2 V (blue) was responsive in the small curvature range. (e) Device responses were less responsive when the curvature sensor was strained in the perpendicular direction (schematics as shown in the left) rather than in a parallel direction (same as in Figure 3).

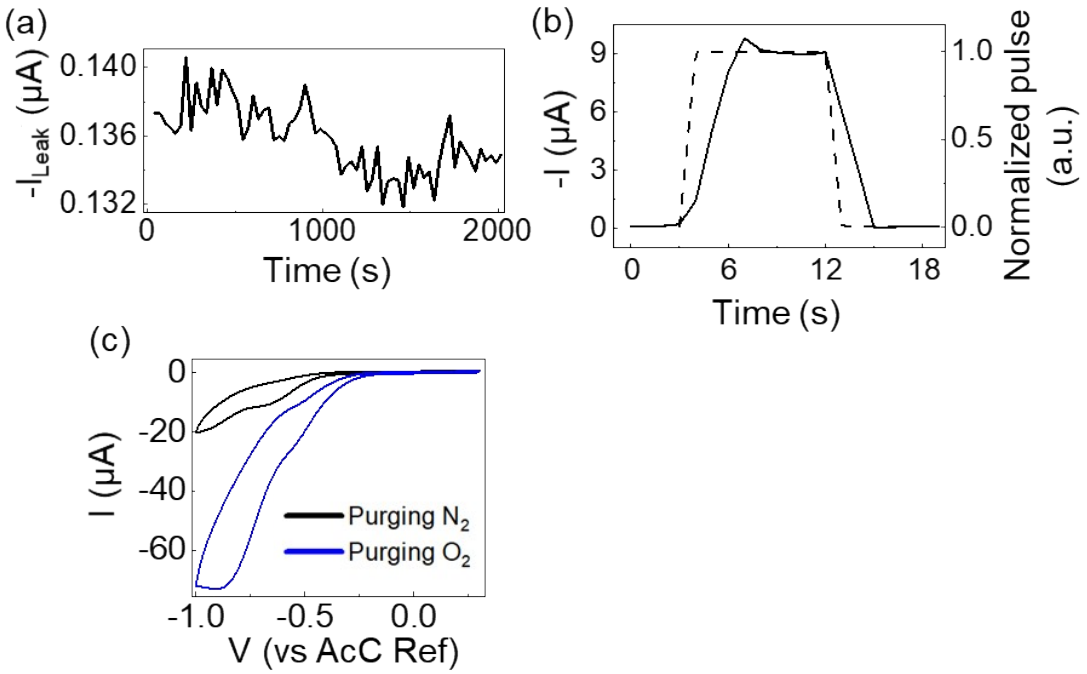

Figure S5. (a) An example of the current noise in the data acquisition channel after integration with the multiplexer circuit. The fluctuations were around 0.01 μA, which was used in calculations of the measurement uncertainty level. (b) Device response time upon switching. The solid line was the device current and the dashed line was the triggering pulse. (c) Current-voltage measurements using a three-electrodes system to sense dissolved oxygen. Based on this redox potential characteristics, the sensor was operated at V = -0.8 V with respect to the reference electrode of activated carbon in the main text.

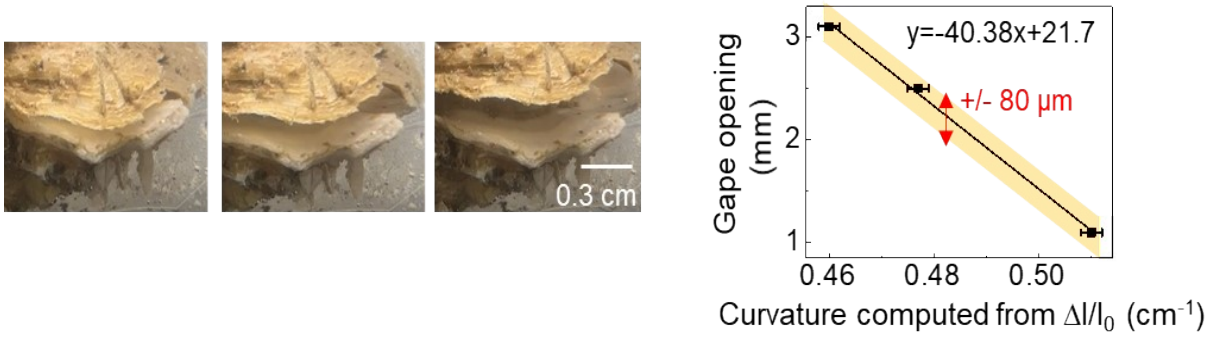

Figure S6. (a) Still-frame photographs of the oyster opening its gape. (b) Correlation of the

gape distance extracted from the photographs with the measurement values from the curvature strain sensor mounted on the oyster shell. The shaded region indicates the uncertainty levels of the measurements.

(a)

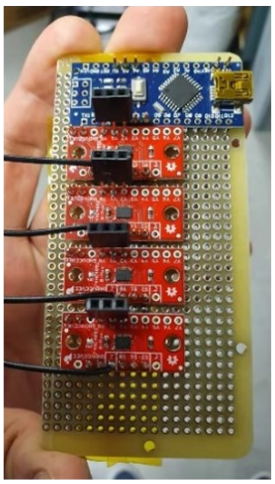

(b)

```
int outputs[4] = {2,3,4};
float receive=20000;
void setup() {
  // put your setup code here, to run once:
  Serial.begin(9600);

  for(int i;i<3;i++) {
    pinMode(outputs[i],OUTPUT);
    }
}

void loop() {
  while (Serial.available()>0)
  {
    String s=Serial.readStringUntil('\n');
    receive=s.toFloat();
    }
  // put your main code here, to run repeatedly:
  Serial.print("channel\t");
  Serial.println(int(receive));
  for(int j=0;j<3;j++){
    for(int i=0;i<3;i++){
      digitalWrite(outputs[i],bitRead(j,i));
       Serial.print(bitRead(j,i));

       }
       Serial.println("");
     delay(receive);
     }
}
```

(c)

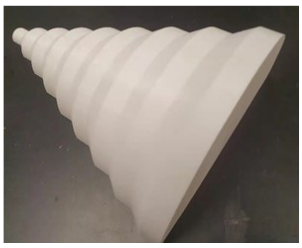

Figure S7. (a) 8-to-1 multiplexer circuits soldered with Nano-Arduino and (b) the control software code. (c) Printed mold for bending the curvature sensor to a calibrated radius of curvature. The model's circular radii range from 9 to 1 cm (right to left).

Reference:

1. Liu, C., Xu, Y. & Noh, Y. Y. Contact engineering in organic field-effect transistors. *Mater. Today* **18**, 79–96 (2015).
2. Cucchi, M. *et al.* Directed Growth of Dendritic Polymer Networks for Organic Electrochemical Transistors and Artificial Synapses. *Adv. Electron. Mater.* **7**, (2021).